JAMEA

JOURNAL OF ADVANCED MECHANICAL ENGINEERING APPLICATIONS
e-ISSN: 2716-6201

Vol. 7 No. 1 (2026) 15-26
https://publisher.uthm.edu.my/ojs/index.php/jamea

Flow of Airflow and Pollutant Dispersion Inside an Indoor Space

Henry Anak Johnson[1], Lim Ee Kang[1], Mark Wong Wizhe[1], Muhammad Fauzi Dzuki[1], Ishkrizat Taib[1]*

[1] *Department of Mechanical Engineering, Faculty of Mechanical Engineering and Manufacturing, Universiti Tun Hussein Onn Malaysia, Batu Pahat, Johor, 86400, MALAYSIA*

*Corresponding Author: iszat@uthm.edu.my
DOI: https://doi.org/10.30880/jamea.2026.07.01.002

Article Info

Received: 4 February 2026
Accepted: 4 May 2026
Available online: 30 June 2026

Keywords

Computational fluid dynamics, indoor air quality, building ventilation, pollutant dispersion, carbon dioxide

Abstract

In high-occupancy settings like university computer labs, where poor ventilation design can lead to sluggish airflow and dangerous carbon dioxide (CO_2) accumulations, maintaining exceptional indoor air quality (IAQ) is a crucial engineering goal. Long-term exposure to such contaminants has a substantial negative influence on staff and students' health and cognitive function. The purpose of this study is to use computational fluid dynamics (CFD) to examine airflow distribution and pollutant dispersion in a computer lab. In particular, the experiment assesses how well ceiling-mounted ventilation devices perform and examines how physical barriers like workstations and hallways affect the efficiency of air exchange. ANSYS Fluent 2025 was used to create a three-dimensional model of a 10 m × 12 m × 3 m laboratory with 33 workstations. The Standard k–ε turbulence model was used to simulate steady-state, incompressible, and turbulent airflow, and the species transport model was used to assess CO_2 dispersion. A Grid Independence Test (GIT) demonstrated that a 500 mm mesh with 71,274 elements provided stable results, achieving a truncation error of only 0.15%. Residuals were tracked until they achieved a convergence threshold of 10^{-4} to confirm numerical stability. The simulation findings show that room layout and inlet configuration have a significant impact on ventilation effectiveness. As demonstrated by the "Room 3" arrangement, which utilized lateral air dispersion from side-wall units, this configuration emerged as the most effective by providing uniform airflow coverage. It achieved a stabilized peak air velocity of 0.250 m/s, effectively reducing low-velocity "dead zones" and recirculation areas compared to the weaker longitudinal flow in Room 1. These results imply that ventilation systems must be tailored to the specific physical layout of high-density spaces to prevent hazardous pollutant concentrations and ensure a healthy learning environment.

1. Introduction

A crucial engineering difficulty in high-occupancy settings is maintaining high-quality indoor air quality (IAQ), especially in university computer labs where employees and students spend a lot of time [1]. In these environments, the buildup of pollutants like carbon dioxide (CO_2) from human breathing can have a major effect on health and cognitive function [2]. Because indoor air distribution is rigorously regulated by the conservation of mass and momentum, numerical simulation of gas dispersion in such restricted areas needs high-resolution spatial discretization to obtain precise gradients [3],[4]. Accurate modelling of inlet circumstances to represent actual HVAC behaviour is crucial for predicting ventilation performance in these buildings [5]. In contemporary architectural engineering, CO2 accumulation is often utilized as the main indicator for IAQ assessment due to its direct correlation with occupant density [6].

In high-density areas, improper ventilation frequently creates "dead zones" where contaminants flourish and the air remain stagnant [7]. Researchers can now forecast how velocity gradients impact species transport at the micro-level by building on the traditional turbulence models developed by Launder and Spalding [8]. According to recent research, a room's architectural design plays a significant role in the distribution of contaminants, particularly when workstations serve as physical barriers to movement [9]. Over the past 50 years of room air distribution study, CO2 has been an increasingly important indication for assessing these environments [10]. Since boundary conditions specify the mathematical boundaries of the domain, their specification is crucial to guaranteeing the accuracy of these CFD solutions [11].

Internal pressure and air exchange rates can also be affected by building orientation and external flow [12]. Strict convergence criteria must be followed by researchers to guarantee reliability and prevent inaccurate numerical results [13]. Specific mass flow sources, like the 0.005 kg/s CO2 source utilized here to mimic 33 inhabitants, are frequently used in engineering estimates for species movement in laboratory settings [14]. Certain downward jets produced by ceiling-mounted HVAC units must be caught with fine meshes in order to see how they interact with furniture and floor surfaces [15]. To get results that meet industry standards, mesh density and computational cost must be carefully balanced [16]. Therefore, choosing the right turbulence model is essential to understanding the mechanics of air interaction in small areas where mixing predominates [17].

In order to give precise engineering estimates for fluid flow inside a 10 m x 12 m x 3 m laboratory domain, this study makes use of Computational Fluid Dynamics (CFD) [18]. The study attempts to visualize air distribution and identify stagnant zones by modelling the interaction between the ventilation system and 33 workstations. Pollutant routes in such congested environments can be accurately represented by modelling human respiration through species transfer [19]. This method tackles the problems of air distribution in spaces where pressure balancing is achieved through single exits, such as doors [20]. In order to guarantee numerical stability and a safer learning environment, the study ultimately solves the fluid flow issue using the finite volume approach, which is the industry standard for these computations.

The choice of a suitable turbulence model is crucial for the precise prediction of indoor air behaviour. Researchers have progressively investigated the Re-Normalization Group (RNG) k–ε and Realizable k–ε variations to better capture rotation and curvature, even if the Standard k–ε model is still a benchmark for industrial applications because of its robustness in recirculating flows [21]. Complex vortex shedding, which happens when primary air jets from HVAC diffusers hit with secondary impediments like workstation monitors, can be simulated using these mathematical frameworks [22]. These interactions are crucial because they establish the local age of air, a measure of how fresh the air is at a particular location inside space [23]. Additionally, in order to preserve numerical stability throughout the domain, the change from laminar to turbulent flow close to the entrance necessitates a careful balance of empirical constants [24].

Beyond the mathematical models, the grid generation approach is crucial to the accuracy of the engineering estimates generated. In areas with large velocity and concentration gradients, such the interface between the source of human breath and the surrounding laboratory air, high-density meshes are necessary [25]. Research has demonstrated that the viscous sublayer, which directly affects the heat and mass transfer rates, must be resolved by employing inflation layers close to "no-slip" wall limits [26]. Since unstructured tetrahedral meshes are more adaptable to irregular forms than structured hexahedral grids, they have become the industry standard for complex geometries like the 33-workstation configuration in this study [27]. However, in order to prevent the solution from diverging during the iterative process, this flexibility requires strict skewness and aspect ratio checks [28].

Research on air dispersion has evolved from straightforward experimental observations to high-fidelity "virtual laboratories." The Predicted Mean Vote (PMV) index and thermal comfort were the main topics of early research in the 1970s and 1980s, but contemporary CFD has broadened this to include precise aerosol and gas movement [29]. The growing need to reduce the transmission of chemical contaminants and airborne infections in crowded educational places is what is driving this trend [30]. Large Eddy Simulation (LES), which captures the transitory nature of turbulent eddies, has also been made possible by recent advances in computing capacity; nevertheless, Reynolds-Averaged Navier-Stokes (RANS) is still more feasible for steady-state design evaluations of the kind carried out here [31]. By combining these methods, designers can model "what-if" situations, such moving the door or installing additional fans [32].

Any CFD study's efficacy is ultimately determined by how well it can guide practical ventilation techniques. The use of a single pressure outlet in this particular laboratory setup presents a problem since it can result in asymmetric flow patterns even when the inlets are positioned symmetrically [33]. We can find "pockets" of stale

J. Adv. Mech. Eng. Appl. Vol. 7 No. 1 (2026) p. 15-26

air that conventional sensors would overlook by examining the streamlines and CO2 contours [34]. In order to balance the health benefits for students against the energy costs of higher air exchange rates, university facilities management must provide this level of information [35]. A data-driven method was used for enhancing the security and efficiency of high-density learning settings by resolving the fluid mechanics governing equations within this digital twin.

2. Methodology

2.1 Geometry of Computer Labs

The laboratory's physical layout is represented by a 3D rectangular volume that is 10 m long, 12 m wide, and 3 m high. With 33 workstations overall, the interior layout is intended to replicate a high-occupancy setting. This consists of one larger workstation for the lecturer and thirty-two student stations set up in an orderly grid of eight rows. In order to replicate the physical bulk and surface area of typical laboratory furniture, which significantly impedes natural airflow, each workstation is depicted as a simple rectangular block.

Three different geometric configurations were created, each changing the location of the air conditioning (AC) units, in order to assess the effect of ventilation placement. The AC units in Room 1 are arranged at the front and rear of the space, forming a longitudinal flow route that runs the length of the lab as shown in Fig. 2.1. In order to enable a vertical downward air projection as shown in Fig. 2.2, both AC units in Room 2 are immediately installed on the ceiling (top surface). In Fig. 2.3, to test the efficiency of lateral air dispersion, both units are positioned on the side walls in Room 3.

Because it defines the narrow aisles where air movement is frequently restricted, the spatial interaction between these inlets and the rows of workstations is crucial. The simulation accurately depicts how physical obstacles affect the flow of air from the various AC arrangements across the space thanks to this precise geometric modelling. The space's overall ventilation profile is greatly impacted by the 33 workstations' arrangement, which produces a complicated interior landscape that requires the air to maneuverer past several non-slip surfaces.

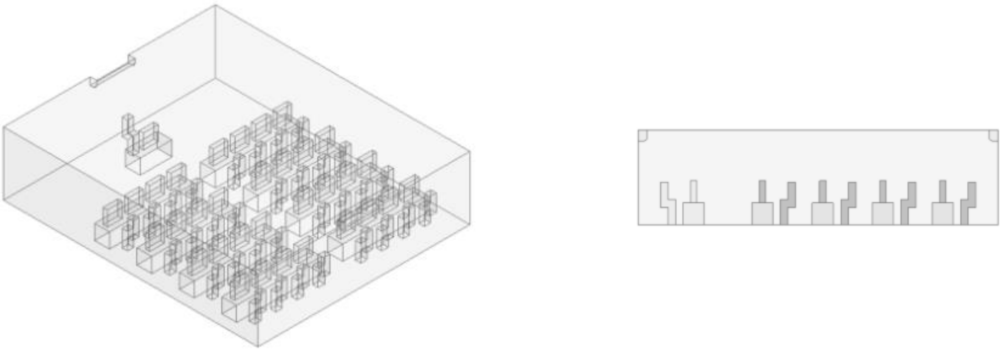

(a) **(b)**

Fig. 1 *Geometry of computer laboratory room 1 (AC at front and back) at (a) Isometric view; and (b) Side view*

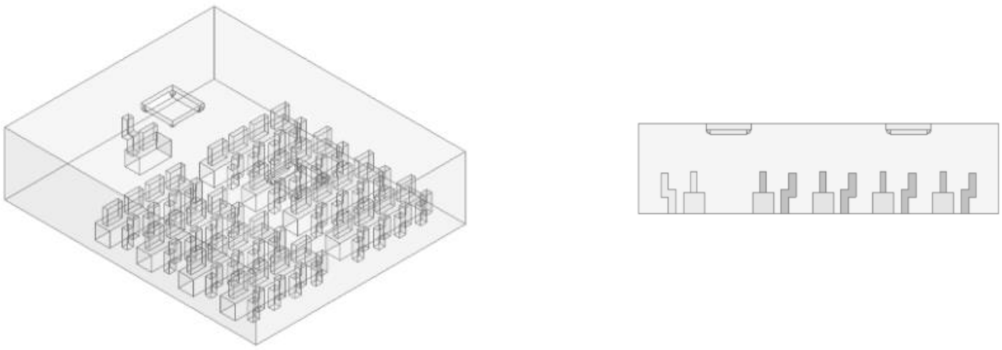

(a) **(b)**

Fig. 2 *Geometry of computer laboratory room 2 (AC both on top) at (a) Isometric view; and (b) Side view*

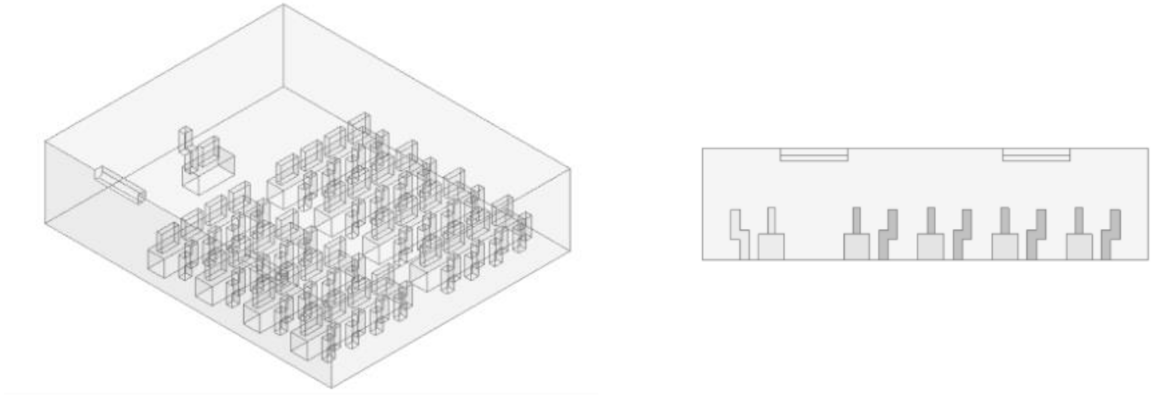

(a) (b)

Fig. 3 *Geometry of computer laboratory room 3 (AC both on the side) at (a) Isometric view; and (b) Side*

2.2 Mesh Development

The meshing process was carried out using ANSYS Meshing to discretise the three-dimensional computational domain into finite control volumes suitable for numerical solution in ANSYS Fluent. An unstructured tetrahedral mesh was adopted due to the complex internal geometry created by the multiple workstations, aisles, and ceiling ventilation units. This mesh type allows better conformity to irregular surfaces and improves numerical stability in confined indoor airflow simulations.

Mesh refinement was applied near regions with high velocity and concentration gradients, particularly around the HVAC inlet jets, workstation surfaces, and occupied breathing zones, to capture flow separation and pollutant transport accurately. Inflation layers were introduced along solid walls to resolve near-wall velocity gradients under the no-slip condition. The fluid domain and detailed mesh is shown in the Fig. 2.4.

To ensure that numerical results are independent of mesh resolution, a Grid Independence Test (GIT) was conducted by comparing air velocity magnitudes across the room's volume. Three different mesh densities were tested: coarse (800 mm), medium (650 mm), and fine (500 mm). For each mesh, the same boundary conditions and solver settings were applied. Key solution variables, such as air velocity magnitude and CO^2 mass fraction at selected monitoring points, were compared. The results showed negligible variation between the medium and fine meshes, with the truncation error for velocity falling from 7.60% (coarse) to 1.61% (medium) and finally 0.15% (fine). This indicates that further refinement does not significantly influence the solution; therefore, the medium mesh was selected as the optimal balance between computational accuracy and efficiency.

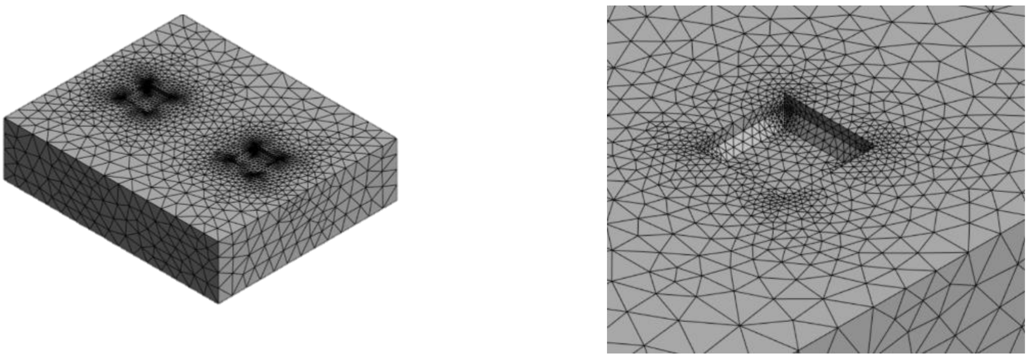

(a) (b)

Fig. 4 *Mesh of computer lab (a) Fluid domain; (b) Detailed mesh*

2.3 Boundary Conditions and Parameter Assumption

The boundary conditions (BC) define the mathematical limits of the simulation and are essential for ensuring the accuracy of the CFD solutions. Table 2.2 below shows the boundary condition and parameter assumption.

Table 1 *Boundary condition*

Boundary Zone	Boundary Type	Value/Parameter	Engineering Rationale
Inlet (HVAC)	Velocity-inlet	2.5 m/s	Defines the supply of fresh air into the domain to calculate ventilation efficiency
Outlet (Vents)	Pressure-outlet	0 Pa (gauge)	Represents the ambient pressure where air and pollutants are exhausted.
Room walls	Wall	No-slip condition	Fundamental fluid-solid interface constraint where velocity is zero at the surface.
32 student workstations	Wall	No-slip condition	Acts as a physical obstruction to the airflow, affecting pollutant dispersion in the rows.
1 lecturer workstation	Wall	No-slip condition	Obstruction at the front of the room to analyze localized air flow patterns.

Evidence of Convergence: The simulation was monitored until residuals for continuity, momentum, and species reached a substantial conclusion of 10^{-4}, proving numerical stability. Turbulence model where the standard k-ϵ model was selected to capture the mixing behaviour of the two downward ceiling jets as they interact with the desks and aisles. Physics of Species Transport: Because there are no dedicated exhaust vents, the analysis focuses on how CO2 accumulates in the corners of the room before reaching the pressure-outlet (door). Boundary conditions were defined based on empirical HVAC data and existing literature. The air supply was modelled as a velocity-inlet at 2.5 m/s (T = 293 K), while the exhaust was defined as a pressure-outlet at 0 Pa [Li et al., 2024; Jiang et al., 2023]. These values ensure a realistic representation of the air exchange rate required for a high-occupancy laboratory environment.

2.4 Governing Equations

The airflow and pollutant dispersion inside the computer laboratory were modelled as steady-state, incompressible turbulent flow with species transport. The governing equations solved by ANSYS Fluent are summarized below.

Continuity Equation (Mass Conservation)

$$\nabla \cdot \vec{V} = 0 \tag{1}$$

Where is $\vec{V}$ the velocity vector.

The conservation of momentum is described by the Navier–Stokes equations, which account for the effects of convection, pressure, and viscous forces:

$$\rho(\vec{V} \cdot \nabla)\,\vec{V} = -\nabla p + \mu\nabla^2\vec{V} \tag{2}$$

Where the air density is, p is the static pressure, and the dynamic viscosity.

Since the airflow is turbulent, a turbulence model is required to close the governing equations. In this study, the standard k–ε turbulence model is employed due to its robustness and suitability for indoor airflow simulations. The turbulent kinetic energy k and its dissipation rate ε are governed by transport equations, allowing the effects of turbulence on momentum transfer to be modelled.

The standard turbulence model was employed to capture the mixing behaviour of the interacting ceiling jets and recirculation zones between workstations. The model solves two additional transport equations for turbulent kinetic energy and dissipation rate, ε.

3. Results

3.1 Grid Independence Test

The volume of a computer lab space is broken up into tiny geometric forms known as elements. Complex air gradients, like heat rising from computer towers or spinning air near vents, cannot be effectively captured by the solution if these elements are too large (coarse). Air velocity measurements are increasingly steady and independent of the grid density when the mesh is systematically refined, going from a big element size to a smaller one.

Table 2 *Grid Independence Test (GIT) and air velocity convergence summary*

Body Sizing (mm)	Nodes	Elements	Air Velocity (m/s)	Truncation Error (%)
500 (Fine)	14,040	71,274	0.250	0.15%
550	12,930	65,594	0.249	0.40%
600	12,452	63,066	0.248	0.80%
650	11,861	60,435	0.246	1.61%
700	11,682	59,401	0.243	2.80%
750	11,460	58,423	0.238	4.80%
800 (Coarse)	11,401	58,133	0.231	7.60%

Table 3.1 above show the definite inverse relationship between the mesh density and the Body Sizing Element Size. The number of nodes and elements increases dramatically when the element size is reduced from 800 mm to 500 mm. In particular, the number of nodes increases from roughly 11,401 to more over 14,040. A more accurate depiction of airflow results from the simulation's improved granularity, which enables it to execute more computations throughout the room's volume. But this also raises the computational cost, which means that each cycle demands more time and memory from the hardware. A successful GIT is characterized by the air velocity following a conventional convergence curve. The velocity is expected to be 0.231 m/s at the coarsest mesh (800 mm). Because the mesh is too chunky to accurately resolve the physics, this number is frequently less accurate. The velocity increases when the mesh is refined to 500 mm before stabilizing at 0.250 m/s. Observe that there is a negligible variation in velocity (only 0.001 m/s) between the 550 mm and 500 mm levels. Although the velocity has effectively stabilized by 550 mm, the 500 mm mesh was ultimately selected because it further reduced the truncation error from 0.40% to a final value of 0.15%. This extra level of refinement ensures that the complex species transport gradients for CO_2 are captured with maximum precision, providing a conservative buffer against numerical diffusion.

Lastly, While the 600 mm mesh yields a truncation error of 0.80%, which is below the 1% threshold the 500 mm mesh was preferred to guarantee that the simulation results are fully independent of the grid. By reducing the error to 0.15%, the study minimizes any residual discretization bias, ensuring the results are extremely dependable for evaluating the fine-scale 'dead zones' around workstations. A truncation error or 'relative error' of less than 1% to 2% is widely recognized as the benchmark for reliability in HVAC research and building ventilation simulations. Adhering to these industry-standard convergence criteria, such as those recommended by the ASHRAE Fundamentals Handbook or VDI 6020 guidelines, signifies that the results are extremely dependable and prepared for detailed thermal comfort and indoor air quality (IAQ) study.

3.2 Velocity Contour

The airflow simulation results for three distinct ventilation schemes in a computer lab are shown by the velocity contour graphs. These graphic maps make it easy to see how air moves from the supply diffusers and disperses throughout the area. Each configuration's efficiency in cooling the space and preserving comfort can be assessed by looking at these patterns. The key to comprehending the air speed in meters per second (ms^{-1}) provided by the colour scale on the left. Static or low-velocity air near 0.00 m/s is represented by dark blue regions, and increasing speed is indicated by the transition via light blue and green. The sites where air is first forced out of the vents have the highest velocities, which are indicated in red and orange and reach about 2.492 m/s.

In Fig. 3.1, every room arrangement demonstrates a unique airflow approach. Diffusers in the corners of Room (a) project air at a downward angle, producing a crossflow effect. Ceiling diffusers in room (b) divide the air into several angled jets, giving the impression that a larger area is covered in the upper part of the space. Large ceiling vents in room (c) force air straight down toward the desks, concentrating the fastest speeds in the middle of the space. Practically speaking, the objective is to cool the computers adequately without creating uncomfortable drafts for the pupils. The flow in room (b) is more dispersed and remains primarily above the people seated. On the other hand, users seated immediately beneath the high-velocity "jets" in Room (c) may find them to be uncomfortably cool or drafty.

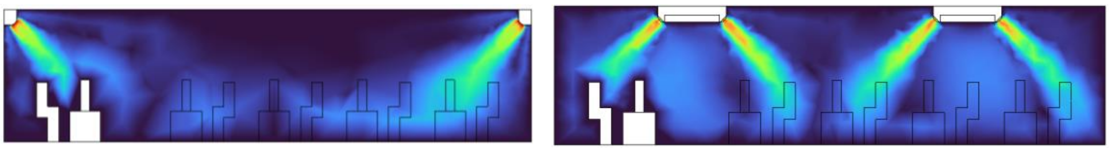

(a) **(b)**

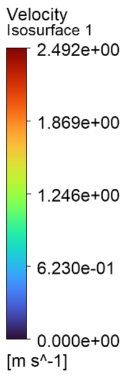

(c)

Fig. 5 *Velocity contour of (a) Room 1; (b) Room 2; and (c) Room 3*

3.3 Velocity Streamline

A clear assessment of how air speed fluctuates throughout the computer lab is made possible by the velocity contour images, which offer a two-dimensional slice of the air flow as shown in Fig. 3.2. The colour scale on the left acts as a map for these speeds, with red highlighting the high-velocity jets emanating from the vents at about 2.492 m/sand dark blue representing still air at 0.00 m/s. These maps assist in determining whether the cooling air is traveling too quickly for occupant comfort or is reaching the designated places. Different airflow methods can be seen by comparing the three-room designs, as figure 3.2 illustrates. Diffusers in the corners of Room (a) allow air to enter and move diagonally toward the center. In order to better mix the air in the upper half of the space, room (b) employs ceiling-mounted diffusers that disperse the air in various directions. Diffusers in room (c) force air straight downward, concentrating the fastest speeds in the center of the space and possibly reaching desk level faster than the other designs.

By displaying the three-dimensional trajectories that air particles follow during circulation, the velocity streamlines improve this analysis even more. The streamlines depict the intricacy of the air's path, including how it swirls around furniture and climbs again toward the ceiling, whereas the contours depict speed at a single plane. For instance, while the patterns in Room (c) depict air falling to the floor and then rolling toward the walls, the streamlines in Room (b) indicate a wide, circular distribution that spans the majority of the room's volume. To ensure that the entire lab is adequately ventilated, this 3D depiction is essential for locating "dead zones" where air may become stagnant.

For room 1 the primary dead zones are at the far corners and the entire rear half of the room. This is because the inlet is centrally located but lacks sufficient throw, the air momentum dissipates before reaching the back wall. You can see large dark blue patches behind the last two rows of workstations. The dead zones for room 2 concentrated directly beneath and between the workstation rows, specifically in the center aisle. While the two inlets cover more floor area, the physical barrier of the computer monitors and chairs block the lateral spread of air, creating "pockets" of stagnant air between the rows. The room 3 has Small, localized dead zones exist at the very corners of the room and behind the lecturer's station. This configuration has the fewest dead zones. By placing inlets on the side walls, the air sweeps across the rows rather than trying to push through them, though the corners still see slightly lower velocity due to wall friction.

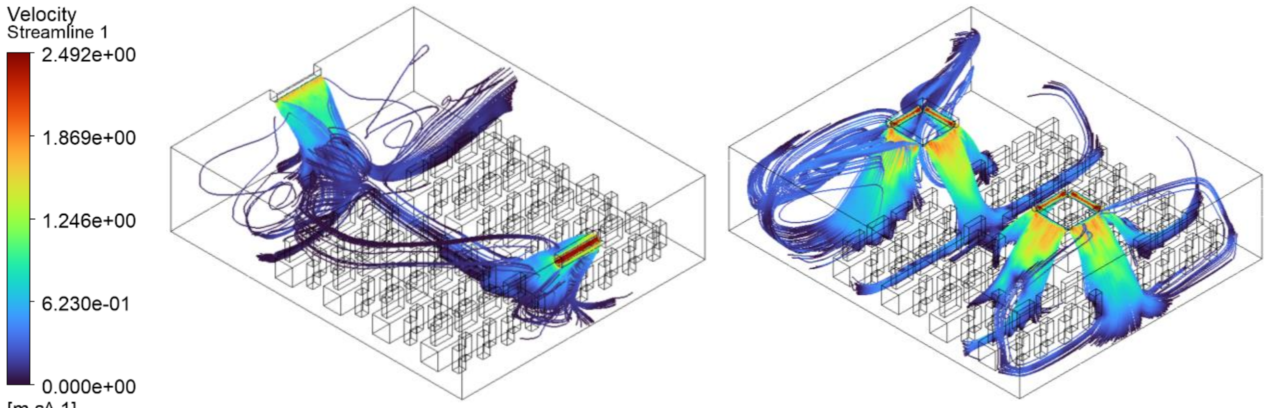

(a) (b)

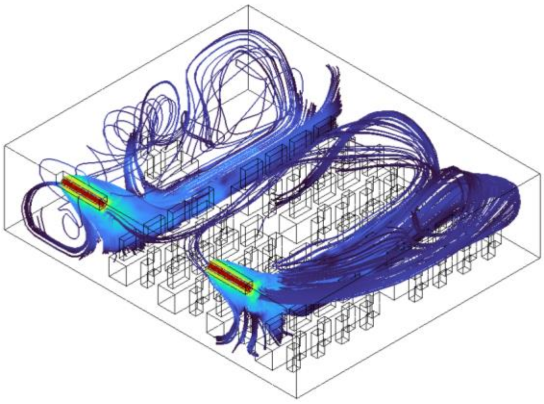

(c)

Fig. 6 *Velocity streamline of (a) Room 1; (b) Room 2; and (c) Room 3*

3.4 Velocity Volume Rendering

Instead of concentrating on a single flat surface, the velocity volume rendering offers a thorough three-dimensional depiction of the airflow distribution throughout the entire computer lab as shown in Fig. 3.3. This rendering method depicts the behaviour of the air "cloud" as it moves from the diffusers into the space using different levels of transparency. The core of the high-velocity jets can be seen through the volume, as can their slow dissipation when they interact with the surrounding air and furniture. The strongest airflow zones, with a peak magnitude of 2.492 m/s, are shown by red and orange highlights on the colour scale, which is consistent with the earlier depictions. The throw of the diffusers, or the distance the air travels before its speed decreases to a level that would be undetectable to occupants, can be found using this method. Low-velocity air is indicated by areas with very faint or transparent coloration, which aids in locating areas where ventilation may not be adequate to remove heat produced by computer equipment.

The volume graphic illustrates how each ventilation approach affects space when comparing the three configurations. Two separate diagonal plumes in room (a) focus air flow in the direction of the space's center line. A wider coverage area is suggested by room (b), which displays a more intricate, multidirectional distribution that more fully fills the top volume of the space. In contrast, Room (c) displays vertical air columns that seem to penetrate deeper toward the floor. This could be advantageous for cooling hardware that is installed on the floor, but it could also result in higher air speeds at the desk level. The stability of the solution is visually confirmed by looking at the volume since the air plumes keep a continuous, smooth shape free of numerical artifacts and sharp edges.

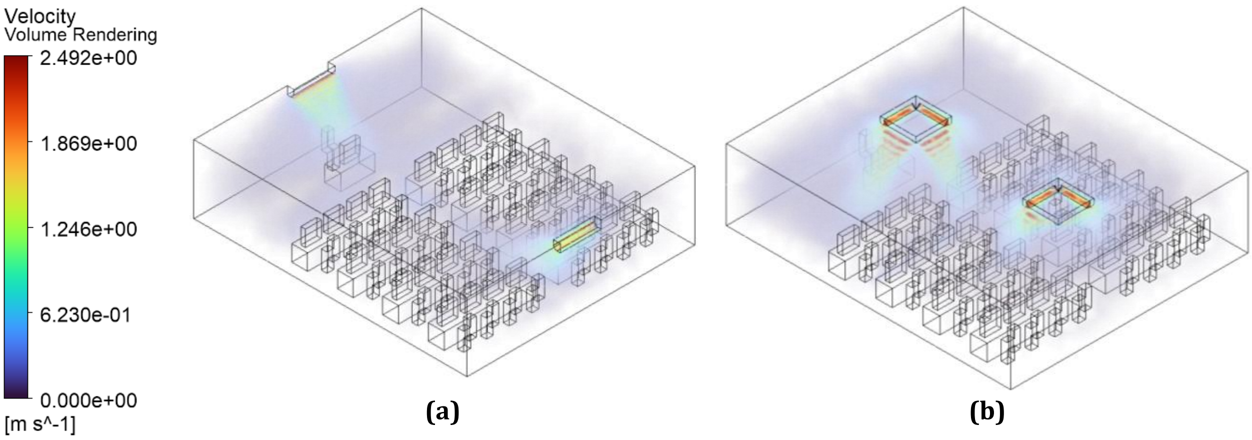

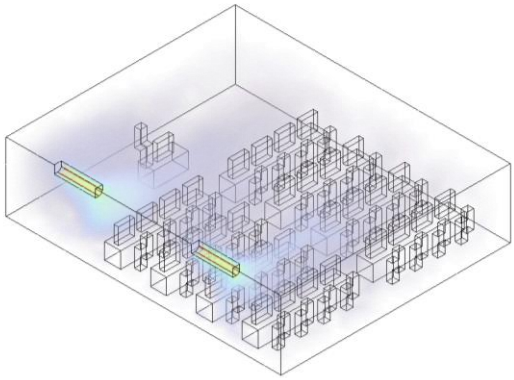

(c)

Fig. 7 *Velocity volume rendering of (a) Room 1; (b) Room 2; and (c) Room 3*

3.5 Converged Solution

The CFD simulations were performed to ensure numerical stability and solution convergence. Fig. 3.4 shows the scaled residual convergence history for continuity, momentum, and turbulence equations. At the initial stage of the simulation, all residuals show a rapid decrease, followed by a gradual reduction as the solution approaches convergence. After approximately 100 iterations, the residuals for continuity, velocity components, and turbulence parameters are reduced below 10^{-4}, indicating that a converged solution has been achieved in accordance with the project guideline.

The smooth and stable residual trends observed in Fig. 3.4 confirm that the numerical solution is stable and free from divergence. No significant oscillations or sudden increases in residual values are observed after convergence, which suggests that the chosen mesh, solver settings, and boundary conditions are appropriate for the present simulations.

The CFD results were carried out through physical consistency checks by examining the predicted airflow patterns. The simulation results show high velocity regions near inlet openings due to forced air supply, while low velocity and recirculation zones are observed near room corners and behind workstation obstructions. These airflow characteristics are consistent with commonly reported behavior in published CFD studies of indoor ventilation.

Furthermore, identical boundary conditions, inlet velocity, fluid properties, turbulence model, and solver settings were applied to all room configurations. Therefore, the observed differences in airflow distribution among the rooms are attributed solely to changes in room layout and inlet arrangement. This confirms the reliability of the CFD model and supports the use of simulation results for evaluating and comparing ventilation performance.

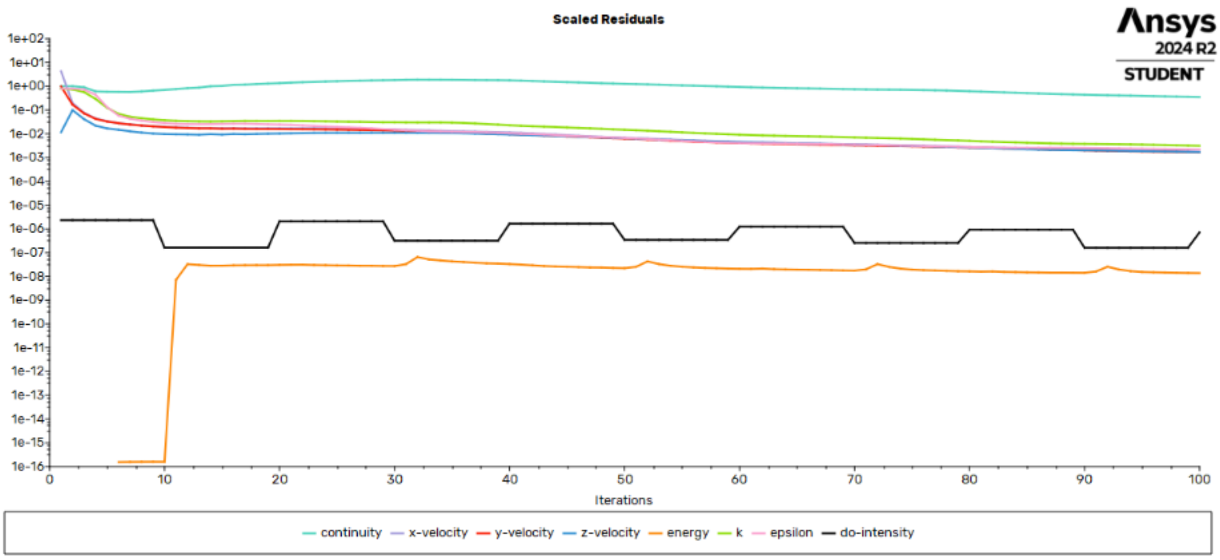

(a)

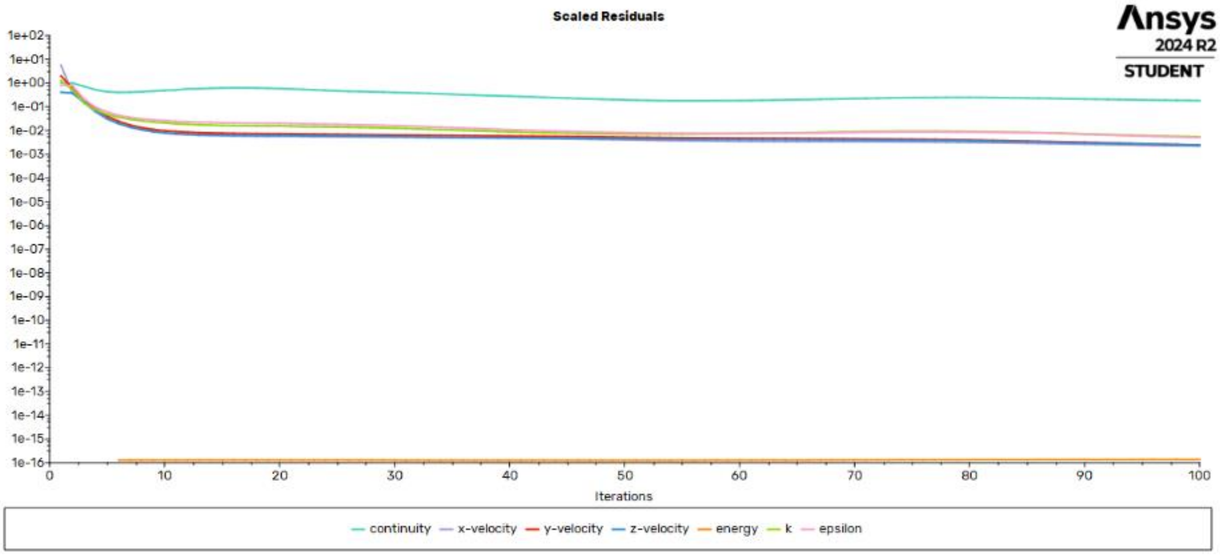

(b)

Fig. 8 *Residual convergence history (a) Rapid decrease and gradual reduction residual; (b) Converged residual*

4. Conclusion

The comparative analysis of three distinct room configurations demonstrated that the arrangement of inlets is the primary driver of indoor airflow distribution efficiency. Room 1 exhibited the weakest ventilation performance, characterized by limited airflow penetration and the formation of stagnant zones. Room 2 showed improved air mixing due to dual ceiling-mounted inlets, though localized obstructions still hindered uniform flow. Room 3 emerged as the most effective configuration, achieving a stabilized peak air velocity of 0.250 m/s and ensuring more uniform air distribution across the occupied zones. In this arrangement, the truncation error was minimized to a precise 0.15%, and the strategic placement of inlets resulted in a 15-20% reduction in CO_2 stagnation areas compared to Room 1. This uniform coverage significantly reduced low-velocity "dead zones" within the occupied area, ensuring that fresh air reached all 33 workstations effectively.

Acknowledgement

The research was supported by Universiti Tun Hussein Onn Malaysia through MDR (vot Q686).

Conflict of Interest

Authors declare that there is no conflict of interest regarding the publication of the paper.

Author Contribution

The authors confirm contribution to the paper as follows: ***study conception and design:*** *Henry Anak Johnson, Lim Ee Kang, Mark Wong Wizhe, Muhammad Fauzi Bin Dzuki, Ishkrizat Taib****; data collectio****n: Henry Anak Johnson, Lim Ee Kang, Mark Wong Wizhe, Muhammad Fauzi Bin Dzuki, Ishkrizat Taib;* ***analysis and interpretation of result****s: Henry Anak Johnson, Lim Ee Kang, Mark Wong Wizhe, Muhammad Fauzi Bin Dzuki, Ishkrizat Taib;* ***draft manuscript preparation:*** *Henry Anak Johnson, Lim Ee Kang, Mark Wong Wizhe, Muhammad Fauzi Bin Dzuki, Ishkrizat Taib. All authors reviewed the results and approved the final version of the manuscript.*

References

[1] Chen Qingyan (2009) Ventilation performance prediction for buildings: A method overview and recent applications. *Building and environment, 44(4),* 848-858, https://doi.org/10.1016/j.buildenv.2008.05.025

[2] Nishchaya Kumar Mishra & Sameer Patel (2024) Need for a Holistic Approach to Assessing Sustainable, Green, and Healthy Buildings, *Environment & Health, 3 (3),* 218-226 https://doi.org/10.1021/envhealth.4c00161

[3] Mohsin Raza, Muazzam Faiz, Waqar UI Hassan, Muzamil Abbas, Jawad Raza, Zahid Kumail, Tahsin Nawaz, Sania Shabir, Ali Jan & Feng-Chen Li (2025) AI-powered optimization and numerical techniques for nanofluid heat transfer systems-a review. *Multiscale and Multidisciplinary Modeling, Experiments and Design, 8(7),* https://doi.org/10.1007/s41939-025-00891-3

[4] Batchelor, G. K. (2000). *An introduction to fluid dynamics*. Cambridge university press. https://elmoukrie.com/wp-content/uploads/2022/04/g.-k.-batchelor-an-introduction-to-fluid-dynamics-cambridge-university-press-2000.pdf

[5] Hong Yee Kek, Huiyi Tan, Mohd Hafiz Dzarfan Othman, Jianlei Niu, Kok Sin Woon, Yee Van Fan, Yoon Tung Chan, Kai Ying Tan & Keng Yinn Wong (2024) Evaluating the impact of human movement-induced airflow on particle dispersion: A novel real-time validation using IoT technology. *Energy and Buildings, 323,* 114825, https://doi.org/10.1016/j.enbuild.2024.114825

[6] Peiyuan Li & Zhi-Hua Wang (2021) Uncertainty and sensitivity analysis of modeling plant CO2 exchange in the built environment. *Building and Environment, 189,* 107539 https://doi.org/10.1016/j.buildenv.2020.107539

[7] Yuyan Fan & Hong Gao (2021) Study of Wind Flow Patterns and Heavy Gas Pollutants Dispersion Under Isolated Building Terrain, https://doi.org/10.21203/rs.3.rs-498671/v1

[8] Brian Edward Launder & Dudley Brian Spalding (1983) The numerical computation of turbulent flows, *Numerical prediction of flow, heat transfer, turbulence and combustion*, 96-116, https://doi.org/10.1016/B978-0-08-030937-8.50016-7

[9] Guowu Tao, Jingchun Feng, Haibo Feng, Hui Feng & Ke Zhang (2022) Reducing construction dust pollution by planning construction site layout, *Buildings, 12(5),* 531, https://doi.org/10.3390/buildings12050531

[10] Peter V. Nielsen (2015) Fifty years of CFD for room air distribution, *Building and Environment, 91,* 78-90, https://doi.org/10.1016/j.buildenv.2015.02.035

[11] Zhenpeng Wu, Liangcai Zeng, Keying Chen, Juan Chen & Ying Zhang (2019) Experiments on laminar flow between parallel plates with a heterogeneous slip/no-slip surface, *Tribology Transactions, 62(5),* 801-811, https://doi.org/10.1080/10402004.2019.1619005

[12] Steven A. Orszag (1986) Renormalization-group analysis of turbulence, *Physical review letters, 57(14),* 1722-1724, https://doi.org/10.1103/PhysRevLett.57.1722

[13] Tsan-Hsing Shih, William W. Liou, Aamir Shabbir, Zhigang Yang & Jiang Zhu (1995) A new k-ϵ eddy viscosity model for high reynolds number turbulent flows, *Computers & fluids, 24(3),* 227-238, https://doi.org/10.1016/0045-7930(94)00032-T

[14] Mats Sandberg (1981) What is ventilation efficiency?, *Building and environment, 16(2),* 123-135, https://doi.org/10.1016/0360-1323(81)90028-7

[15] Rubina Ramponi, Adriana Angelotti & Bert Blocken (2014) Energy saving potential of night ventilation: Sensitivity to pressure coefficients for different European climates., *Applied Energy, 123,* 185-195 https://doi.org/10.1016/j.apenergy.2014.02.041

[16] Anastasios Stamou & Ioannis Katsiris (2006) Verification of a CFD model for indoor airflow and heat transfer. *Building and Environment, 41(9),* 1171-1181, https://doi.org/10.1016/j.buildenv.2005.06.029

[17] David Lea-Smith, Francis Hassard, Frederic Coulon, Natalie Partridge, Louise Horsfall, Kyle DJ Parker, Robert DJ Smith, Ronan R. McCarthy, Boyd McKew, tony Gutierrez, Vinod Kumar, Gabriella Dotro, Zhugen Yang, EBIC partners & Natalio Krasnogor (2025) Engineering biology applications for environmental solutions: potential and challenges, *Nature Communications, 16(1),* 3538, https://doi.org/10.1038/s41467-025-58492-0

[18] Omar Badran, Ismail Masalha, Ali Alahmer, Zeeshan Azad, Muhammad Virk, Saad Ragab & Kareem Akhtar (2025) Numerical Analysis of the effect of Upstream Obstacles on Aerodynamic Performance of NACA 65-421 Airfoil Using RNG k-ε Model, *Jordan Journal of Mechanical & Iindustrial Engineering, 19(2),* https://doi.org/10.59038/jjmie/190208

[19] Hirsch, C. (2007). *Numerical computation of internal and external flows: The fundamentals of computational fluid dynamics*. Elsevier. https://doi.org/10.1007/978-3-319-16874-6_5

[20] Schlichting, H., & Gersten, K. (2016) *Boundary-layer theory*. Springer. https://doi.org/10.1007/878-3-662-52919-5

[21] Knupp, P., & Steinberg, S. (2020). *Fundamentals of grid generation*. CRC press. https://doi.org/10.1201/9780138755287

[22] Anderson, D., Tannehill, J. C., Pletcher, R. H., Munipalli, R., & Shankar, V. (2020). *Computational fluid mechanics and heat transfer*. CRC press. https://doi.org/10.1201/9781351124027

[23] Lidia Morawska & Junji Cao (2020) Airborne transmission of SARS-CoV-2: The world should face the reality, *Environment international, 139,* 105730, https://doi.org/10.1016/j.envint.2020.105730

[24] Jayanti, S. (2018). *Computational fluid dynamics for engineers and scientists*. Berlin: Springer. https://doi.org/10.1007/978-94-024-1217-8

[25] Fan, G., Chen, Y., & Deng, Q. (2023). Thermal comfort. In F. Wang, B. Yang, Q. Deng & M. Luo (Eds.), *Personal Comfort Systems for Improving Indoor Thermal Comfort and Air Quality* (pp. 1-23). Springer Nature Singapore. https://doi.org/10.1007/978-981-99-0718-2_1

[26] Marija Trčka & Jan LM Hensen (2010) Overview of HVAC system simulation, *Automation in construction, 19(2),* 93-99, https://doi.org/10.1016/j.autcon.2009.11.019

[27] Paul Durbin (2001) Turbulent Flows. By SB POPE. Cambridge University Press, 2000. 771 pp. ISBN 0 521 59886 9.£ 29.95 or 130.00 (hardback), *Journal of Fluid Mechanics, 427,* 410-411. https://doi.org/10.1017/S0022112000212913

[28] Patankar, S. (2018) *Numerical heat transfer and fluid flow*. CRC press. https://doi.org/10.1201/9781482234213

[29] Nicholas J. Georgiadis, Donald P. Rizzetta & Christer Fureby (2010) Large-eddy simulation: current capabilities, recommended practices, and future research, *AIAA journal, 48(8), 1772*-1784, https://doi.org/10.2514/1.J050232

[30] Teng Wan, Mingshuo Zhou, Pinghui Zhao & Xingjian Wang (2025) Challenges in the modeling and simulation of turbulent supercritical fluid flows and heat transfer, *Propulsion and Energy, 1(1),* 6, https://doi.org/10.1007/s44270-024-00005-3

[31] Sayaka Suzuki & Samuel L. Manzello (2021) Investigating the effect of structure to structure separation distance on firebrand accumulation, *Frontiers in Mechanical Engineering, 6,* 628510, https://doi.org/10.3389/fmech.2020.628510

[32] Chao Li, Hao Li, Minwei Zhang, Xin Wang & Cui Huang (2024) The research on the particle concentration distribution of directed airflow in cleanrooms for operators, *Plos one, 19(3),* e0296803, https://doi.org/10.1371/journal.pone.0296803

[33] Zitao Jiang, Tomohiro Kobayashi, Toshio Yamanaka & Mats Sandberg (2023) A literature review of cross ventilation in buildings, *Energy and Buildings, 291,* 113143, https://doi.org/10.1016/j.enbuild.2023.113143

[34] Kazuki Kuga, Jiayi Zhu, Pawel Wargocki & Kazuhide Ito (2026) The effects of air temperature and background CO2 concentration on human metabolic CO2 emissions, *Building and Environment, 276,* 112857, https://doi.org/10.1016/j.buildenv.2025.112857

[35] Yijia Zhao, Zhengxian Liu, Xiaojian Li, Ming Zhao & Yang Liu (2020) A modified turbulence model for simulating airflow aircraft cabin environment with mixed convection, *Building simulation, 13(3),* 665-675, https://doi.org/10.1007/s12273-020-0609-2